SPACE RESEARCH INSTITUTE

Academy of Sciences, U S S R

D-218

K.I. Gringauz, M.I. Verigin

ELECTRON TEMPERATURE RADIAL DISTRIBUTION IN SOLAR WIND AND SOLAR WIND MODELS

Moscow

ACADEMY OF SCIENCES OF THE USSR

SPACE RESEARCH INSTITUTE

K.I. Gringauz, M.I. Verigin

ELECTRON TEMPERATURE RADIAL DISTRIBUTION IN SOLAR WIND AND SOLAR WIND MODELS

Moscow, 1975

I. Introduction

As a result of processing the experimental data on plasma electron component obtained on-board the "Mars-3" space vehicle in 1971-1972 a radial dependence of the electron mean temperature in the solar wind at distances from 1 to 1.5 a.u. was determined [1]. A considerable part of the results on electron temperature T_e, published earlier, was obtained by means of the American Earth satellites Vela, OGO, IMP 2-4, i.e. at heliocentric distances $r \sim 1$ a.u. The solar corona temperature data are also available. However, the data on the temperature radial distribution in the region nearest to the Sun, in which the coronal plasma transforms into the solar wind are not available, as well as the data on T_e measurements at the heliocentric distances r differed from 1 a.u. have not been published up to the present.

The many theoretical models of the solar wind [5-7] are the result of the attempts to select the most essential physical processes occuring during the solar corona expansion and to evaluate their influence on the radial distribution of the solar wind parameters. However, a reasonable agreement of the model with the data on the characteristics of plasma

in the solar corona base and near the Earth's orbit can be reached by not a single way using the different assumptions on the physical processes in the solar wind; and for a choice (or creation) of the theoretical model corresponding to the main characteristics of the real solar wind, the direct measurements of these characteristics at different distances from the Sun are required [5-7] . In particular, it is important to know the radial distribution of T_e , since in the solar wind the heat transfer by the convection and heat conduction is basically determined by electrons.

The main purpose of the present paper is a brief review of some available models for the solar wind, the description of the plasma electron component experiment carried out on-board the "Mars-3" and the comparison of the obtained results with the available models of the solar wind. In so doing reviewing the solar wind models, we restrict ourselves to the stationary two-fluid models keeping in mind the possibility of comparison of the obtained radial dependence of mean electron temperature with the calculated one since $T_e \neq T_p$ [6] in the real solar wind, that does not correspond to the one-fluid models.

II. Electron temperature radial distribution in some solar wind models

The model by P.A. Sturrock and R.E. Hartle [8, 9] was the first proposed solar wind model that considered the solar corona expansion in the two-fluid approximation. They have paid attention to the fact that for collisional processes to balance T_e electron and T_p proton temperatures it is necessary that the characteristic time of energy exchange between

electrons and protons $\tau_e \simeq 2.56 \cdot 10^2 T_e^{2/3} (\lambda \cdot n)^{-1}$ should be much less than that of the solar wind expansion $\tau_{exp} = -\frac{n}{v}\left(\frac{dn}{dr}\right)^{-1} \approx \frac{r}{2V}$, where V is a radial component of the solar wind velocity; n is ion or proton concentration; $\lambda = \ln\left[\frac{3(KT)^{3/2}}{2\pi^{1/2} e^3 n^{1/2}}\right] \approx 20$ is a Coulomb logarithm; K is a Boltzmann constant; e is an electron charge. With the mean values of the solar wind parameter $n = 7$ cm^{-3}, $V = 410$ km.sec.$^{-1}$ in the Earth's vicinity [6] it is necessary that T_e should be much less than $\sim 2 \times 10^{30}$K for the condition of electron and proton thermal equilibrium to be fulfilled, but it obviously does not take place.

For the stationary spherically symmetrical expansion of the solar corona P.A. Sturrock and R.E. Hartle numerically solved the following set of the equations neglecting the viscosity and the magnetic field influence:

the continuity equation

$$n V r^2 = J = const , \qquad (1)$$

the equation of motion

$$n m_p V \frac{dV}{dr} = -\frac{d}{dr}\left[nK(T_e + T_p)\right] - \frac{G M_\odot m_p n}{r^2} , \qquad (2)$$

and heat balance equation for electrons and protons

$$\frac{3}{2} nKV \frac{dT_e}{dr} - K T_e V \frac{dn}{dr} - \frac{1}{r^2}\frac{d}{dr}\left(r^2 K_e \frac{dT_e}{dr}\right) = -\frac{3}{2}\nu_E nK(T_e - T_p) , \qquad (3)$$

$$\frac{3}{2} nKV \frac{dT_p}{dr} - K T_p V \frac{dn}{dr} - \frac{1}{r^2}\frac{d}{dr}\left(r^2 K_p \frac{dT_p}{dr}\right) = \frac{3}{2}\nu_E nK(T_e - T_p) , \qquad (4)$$

where K_e and K_p are the electron and proton heat conductions; V_E is a velocity of energy exchange between electrons and protons; m_p is a proton mass; $4\pi J$ is a full flux of electrons or protons from the Sun;

$G\ (= 6.67 \times 10^{-8}\ dyn \cdot cm^{-2} g^{-1})$ is a gravitational constant; $M_\odot\ (= 1.99 \times 10^{33}\ g)$ is the solar mass. Heat conductions and the velocity of energy exchange were taken in the following form:

$$\nu_e = \frac{4(2\pi)^{1/2} n e^4 \lambda}{3(m_e)^{1/2}(K T_e)^{3/2}},$$

$$\kappa_e = 3.16 \frac{nK^2 T_e}{m_e \nu_e},\quad \kappa_p = 3.9 \frac{nK^2 T_p}{m_p \nu_p},\quad \nu_E = \frac{2m_e}{m_p}\nu_e,\quad \nu_p = \frac{4\pi^{1/2} n e^4 \lambda}{3(m_p)^{1/2}(K T_p)^{3/2}} \quad (5)$$

T_{eo} , T_{po} , n_o were prescribed as the boundary conditions at the fixed distance $r = r_o$, i.e. the requirements for the solution to be passed through the critical point and also $T_e \to 0$, $T_p \to 0$ with $r \to \infty$ With the choice of $T_{eo} = T_{po} = 2 \cdot 10^6\ ^\circ K$ and $n_o = 3 \cdot 10^7\ cm^{-3}$ at $r = r_\odot$ (the solar radius) a critical point of the solution was obtained with $r = 7.1\ r_\odot$.

$T_e(r)$ and $T_p(r)$ dependences obtained in [9] under such boundary conditions are presented in Fig. 1. In the Earth's orbit vicinity ($r = R_E = 1.5 \times 10^8\ km = 215\ r_\odot$) $T_e = 3.4 \times 10^5\ ^\circ K$, $T_p = 4.4 \times 10^3\ ^\circ K$, $V = 250\ km \cdot sec^{-1}$, $n = 15\ cm^{-3}$. The temperature radial dependence in this model with $r = R_E$ can be described by the power law with the following exponents: $T_e \sim r^{-2/7}$, $T_p \sim r^{-6/7}$,

R.E. Hartle and A. Barnes [11] tried to eliminate the divergence between the very high T_e values and the T_p low values and the V values in the Earth's vicinity obtained in the model of [9] with the experimental magnitudes of $T_e = 1.3 \times 10^5\ ^\circ K$, $T_p = 4.6 \times 10^4\ ^\circ K$ in the quiet solar wind with $V \approx 350$ km.sec^{-1} [6] by means of the introduction into Eqs. (3, 4) $\mathcal{P}_e$, $\mathcal{P}_p$ terms which describe the additional collisionless plasma heating. They took $T_{eo} = 1.5 \times 10^6\ ^\circ K$, $T_{po} = 1.2 \times 10^6\ ^\circ K$ $n_o = 1.5 \times 10^6\ cm^{-3}$ with $r = 2 r_\odot$ as the boundary

conditions, that have been obtained at this distance in the model [9] . The terms describing the heat sources were taken in the following form:

$$\mathcal{P}_e = 0, \quad \mathcal{P}_p = D_0 (n/n_0) \exp\left[-(r/r_0 - a)^2/b^2\right],$$

where D_0 , a , b are the parameters describing the intensity, the position and the heating source width, respectively. In Fig. 2 the solid lines show $T_p(r)$ dependences calculated with $a = 2$, $b = 22$, $D_0 = 6 \times 10^{-9}$ and $a = 2$, $b = 26$, $D_0 = 3 \times 10^{-9}$. The dotted lines of this Figure correspond to $T_e(r)$ and $T_p(r)$ dependences taken from [9] . $T_e(r)$ dependence in [11] is close to that obtained in [9] and is not shown in Fig. 2. It is seen from Fig. 2 that in the vicinity of the Earth's orbit $T_p(r)$ in this model [11] noticeably exceeds of 9 but as well as in [9] ,

J.V. Hollweg [12] considered the solar wind model where Alfven waves propagating from the Sun along the spiral interplanetary magnetic field are the additional source of energy. The direct acceleration of the solar wind by these waves is described by an addition term of Eq. (2) $-\frac{d}{d^2}\left(\frac{\overline{\delta^2 B^2}}{8\pi}\right)$, where $\overline{\delta^2 B^2}$ is a mean square amplitude of fluctuations of the interplanetary magnetic field B. Near and far from the Sun waves do not practically decay and their propagation is described under VKB -approximation. In the intermediate region it is assumed that due to the Landau non-linear decaying the limitation of the level of the fluctuations $\overline{\delta B^2}/B^2$ occurs (= 1/2 as it is sometimes observed in the solar wind at 1.0 a.u. 13). Based on this assumption and supposing $\mathcal{P}_p = 0$ an additional source of ion heating $\mathcal{P}_p$ can

be calculated in the region considered. Also, [12] analyzes the decrease of the radial component of heat flux due to electron thermoconductivity because of increasing of "a spiral angle" ψ between $\vec{B}$ -vector and radius-vector ($\kappa_e = \kappa_e \cdot \cos^2\psi$ in Eq. (3)). Fig. 3 gives the radial dependence of $T_e(r)$ and $T_p(r)$ calculated in J.V.Hollweg's model [12] under the following boundary conditions: at $r = 2r_\odot$: $n_o = 1.8 \times 10^6\ cm^{-3}$, $T_{po} = 1.2 \times 10^6\ ^oK$, $T_{eo} = 1.5 \times 10^6\ ^oK$. The energy flux density values of Alfven waves at $r = r_o$ for the dependences given above are the following: $0.6 \times 10^4\ erg\ cm^{-2}\ sec^{-1}$ (solid curves); $1.2 \times 10^4\ erg\ cm^{-2}\ sec^{-1}$ (long dotted lines) and $2.4 \times 10^4\ erg\ cm^{-2}\ sec^{-1}$ (short dotted lines). The inherent peculiarity of $T_e(r)$ dependence is that in the Earth's vicinity T_e decreases much more slower than $r^{-2/3}$ since the spiral magnetic field attempts to "lock" the electron thermal flux. The increase of the energy flux of Alfven waves leads to growing of V and, therefore, to decreasing of a "spiral angle" ψ and "locking" the electron heat flux; the decrease rate of T_e at 1 a.u. increases in this case (see Fig. 3).

The application of magnetohydrodynamical waves of the solar origin is not the only way to heat protons and increase the solar wind velocity in comparison with the calculation results in [9] . A.J. Handhausen [14] suggested that the well agreement between the theory and the experiment can be obtained if κ_e electron thermoconduction is decreased as compared to its classical value (see, e.g. [10]) and if the heat interaction between the electron and proton components of the

solar wind is simultaneously enhanced.

The empirical constant factors α , β , γ defining the values $K_e^* = \alpha K_e$, $K_p^* = \beta K_p$, $\nu_E^* = \gamma \nu_E$ were introduced into the set of Eqs. (1) - (4) for the two-fluid model of the solar wind (in [15-16]). Fig. 4 shows the solar wind models calculated in [16] under the following boundary conditions at $r = r_0$: $T_{e0} = T_{p0} = 2.08 \times 10^6$ °K , $n = 10^7$ cm^{-3} . The curves marked with number 1 were calculated with the classical values of the transport coefficients, with number 2 done with $\alpha = 0.25$, $\beta = 1$, $\gamma = 30$ and number 3 with $\alpha = 0.18$, $\beta = 2.3$, $\gamma = 1$. It is seen from this Figure that the modification mentioned above of the transport coefficients leads to simultaneous increasing of T_p and decreasing T_e as compared with the model of [9] . The fall rate of $T_e(r)$ also increases at $r = 1$ a.u. $T_e \sim r^{-m}$ with $m \approx 0.6$.

The two-fluid model of the solar wind with taking into account of the influence of the magnetic field and a viscosity on the solar corona expansion has been considered by C.L.Wolf, J.C. Brandt, R.G. Southwick [17] . The introducing of the viscosity into the equation allows to avoid the singularity in a critical point used in the models considered earlier. In [17] the thermoconduction decrease is provided by the factor $(r/r_0)^\rho \cos^2\psi$ taking into account the influence of the magnetic field "spiral angle" growth and the thermoconduction coefficient diminution. The coefficient ρ was considered as a free parameter for the model to be better suitable to the experimental data. Fig. 5 gives the calculated dependence $T_e(r)$, $T_p(r)$ in the model [17] obtained with

$\rho = -0.728$. In this case in the Earth's orbit the electron thermoconduction decreases by 50 times as compared to the classical one. The calculated parameters of the solar wind on the Earth's orbit: $V = 303\ km \cdot sec^{-1}$, $T_e = 203 \times 10^3\ ^oK$, $T_p = 4 \times 10^4\ ^oK$, $n = 9\ cm^{-3}$ are in rather good agreement with their values in the quiet solar wind. As it is seen from Fig. 5 in the Earth's vicinity $T_e(r)$ decays essentially faster than $r^{-2/7}$ (approximately $T_e \sim r^{-1}$).

III. The experiment description and the "Mars-3" measurement results of the solar wind plasma electron component

At the Earth-Mars flight trajectory of the "Mars-3" space vehicle the measurements of a plasma electron component were carried out by means of an integral electron trap. The principal scheme and the main geometric dimensions of the trap used are shown in Fig. 6. As it is seen from this Figure the electron trap has four electrodes: the analyzing interval is formed by two spherical grids 3-4 and two electrically connected flat grids 5 serve as an electrostatical screen. The trap collector is flat. The curves for electron deceleration are determined over 14 readings (for each curve) of the collector current I_e registered by the instrument $(5.5 \times 10^{-13}\ a \lesssim I_e \lesssim 1.55 \times 10^{-9}\ a)$ when retarding potential $(0 \lesssim E_T \lesssim 400\ v)$ is applied to the analyzing grids 3-4. Almost throughout the flight trajectory the retardation curves were obtained for about 50 sec every 20 min. The instrument sensitivity for the isotropic electron flux taking into account the characteristics of the trap, the amplifier

and the telemetry system was about 0.9×10^{6} $cm^{-2}.sec.^{-1}.sterad^{-1}$.

On board the "Mars-3" the electron trap was installed at the non-sunlit side of the vehicle with the distance from terminator $> 10^{2}$ cm; its axis was oriented in the anti-solar direction within $\pm 1^{0}$. The electron temperature determination from a retardation curve was performed by means of choosing the calculated retardation curves that are the closest to those registered from this vehicle. The calculated curve was computed using the results of the laboratory test of a sensor in quasi-energetical beams of ions Ar^{+} under the assumption of the Maxwell isotropic distribution of electrons in the coordinate system moving with the plasma transport velocity V (= 450 km.sec.$^{-1}$). The variation of V from 300 km.sec.$^{-1}$ to 600 km.sec^{-1} will lead to an error of the order of about 5% appearing in the process of T_e determination. The experiment design is described in detail in [18] and the technique of processing and the estimation of accuracy of the results obtained are done in [19] .

The systematical determination of the solar wind characteristics from the various space vehicles (V , n , T_p , T_e , $\vec{B}$) showed the existence of the significant variations of the parameters mentioned (see, e.g., review [20]). In this case though some peculiarities in the variation of the solar wind parameters associated with the existence of long-lived fluxes are on from one solar rotation to another the significant change of the amplitude and the form of these repeated events occurs but some of them do not repeate at all [20] .

Fig. 7 shows the averaged (over 3-hour intervals) values

of T_e obtained from the "Mars-3" measurement data during the three seccessive rotations of the Sun. It is seen from this Figure that some peculiarities in electron temperature remain during two rotations, at least. Hence, to limit the effects associated with the Sun's rotation in determining $T_e(r)$ the measurement results were averaged over -time (~ 27 days, the Sun's rotation). Such an averaging allows to get rid of the temperature variations having the characteristic times $\lesssim \tau$, i.e. to single out the slowly changing part of T_e (the analog of low-frequency filtering in radioengineering). The similar averaging was also used in determining the radial dependences $B(r)$ by P.J. Coleman et al. [21] and $n_p(r)$ by M. Neugebauer and C.W. Snyder [22] .

Fig. 8 gives histograms of T_e for the periods of the measurements corresponding to the Sun's rotations N 1887 and 1893 when the "Mars-3" was on an average at distances 168×10^6 km and 220×10^6 km, from the Sun respectively. It is seen from the Figure that when the space vehicle removes from the Sun the decrease of the averaged (over the Sun's rotation) temperature of electrons $\bar{T}_e$ and the shift to the lower values of the most probable magnitude of electron temperature T_e^m take place for the same Sun's rotation. The time dependence of heliocentric distance to the "Mars-3" at the flight trajectory is given in Fig. 9.

Fig. 10 presents on a bilogarithmic scale T_e values depending on $\bar{r}$ -heliocentric distance to the "Mars-3" in the middle of the T_e data array available (and used) for the Sun's rotations from N 1886 to 1893 (except the rotation N 1892 at which the comparatively small amount of the measure-

ments of T_e was obtained only at the beginning and at the end of the appropriate period). The dashed lines on the space vehicle trajectory shown in Fig. 9 single out the time intervals adequate with the Sun's rotations mentioned above and the circles on these intervals give the used values of $\bar{r}$. The index m and T_e value at 1.0 a.u. can be defined by the least square method under the assumption of the exponential dependence $\bar{T}_e(r) = \bar{T}_e(R_e)\left(\frac{R_e}{r}\right)^m$ according to the points plotted in Fig. 10. In doing this the "width" of the hystogram of T_e -values for one solar rotation and the number of single T_e -measurements during this period were approximately taken into account by introducing of an optimized sum of squared "weight" values into each term; the sum being proportional to $N_j \times \left(\sum_{i=1}^{N_j} (T_{ei} - \bar{T}_e)^2\right)^{-1}$, where N_j is the number of measurements for the i-th rotation of the Sun. In this respect the following empirical formula $T_e \approx 120 \cdot \left(\frac{R_e}{2}\right)^{0.5} \cdot 10^3$ °K [1] best fits the measurements. The dependence obtained is shown by the solid line in Fig. 10.

Note a comparatively wide spread of experimental data in Fig. 10, obviously related to the time variations in the solar corona base that occur with characteristic times $> \tau$. The above mentioned spread affects the determination of $T_e(r)$ -dependence (inder m) and makes more complicated a direct comparison of experimental data to models of the stationary solar wind. Fig. 8 also shows that, in comparison with T_e -values, most probable T_e^m -values decrease more rapidly with the distance from the Sun. The estimates of radial dependence of most probable T_e yield $T_e^m \sim r^{-0.7}$, and the difference in m determined from average ($m \sim 0.5$) and most probable ($m \sim 0.7$) T_e -values can be obviously

used as a criterion of accuracy obtained from radial $T_e(r)$ dependence measured on the same spacecraft. To determine the radial dependence more accurately in the quiet solar wind, the sample data of systematic observations on-board the spacecraft at a large distance from each other should be used.

IV. Discussion on results

The results of electron temperature measurements on-board Mars 3, given in [1] and in this paper, and those of other T_e -measurements can be compared only for T_e -values near the Earth's orbit $[T_e(R_E)]$. Various earth satellites yield the following values of T_e : Vela-4 (May 1967 - May 1968) - 140.10^{3}°K [6], OGO-5 (March, 1968) - 155.10^{3}°K, IMP-6 (March-June, 1971) - 133.10^{3}°K [4] .

Measurements on Vela-4 and IMP-6 were carried out by one and the same group of authors with similar instruments, i.e. a hemispherical electrostatic analyzer; another group made measurements on OGO-5 using a different instrument (a 3-axis analyzer with initial acceleration of electrons). This fact as well as a relatively short period of measurements [3] might cause the considerable difference in the results obtained by the both groups. The value $\bar{T}_e(R_e) \sim 120.10^{3}$°K according to Mars-3 data from July 1971 to January 1972, i.e. in the period close to that of IMP-6 measurements, is similar to $\bar{T}_e(R_E)$ value from the latter satellite despite the difference in the measuremental methods.

The experimental value of T_e fall rate $\sim r^{-0,5}$ obtained on board Mars-3 substantially exceeds, for larger distance from the Sun, the fall rate of T_e from the solar

wind models of Stirrock and Hartle [9] , Hartle and Barnes [11] and Hallweg [12] , $T_e(r) \sim r^{-2/7}$ in [9, 11] models; $T_e \sim r^{-m}$, $m < 2/7$ (see Fig. 1-3) in [12] models. To compare $T_e(r) \sim r^{-2/7}$ radial dependence [9, 11] with the results of Mars-3 T_e measurements, a dashed line is drawn in Fig.10 that corresponds to the exponential dependence with $m = 2/7$. As mentioned above the dashed line best corresponds to the experimental points in Fig. 10 for a fixed index $m = 2/7$. Fig. 10 shows that with r increasing T_e values decrease faster than it can be expected from the exponential dependence $T_e \sim r^{-2/7}$.

So, in the solar wind models [9, 11] calculated with classic values of electron heat conductivity and of the rate of energy exchange between electrons and ions as a basis the radial dependence of electron temperature does not agree with that experimentally observed on Mars-3. The taking into account of the additional heat inflow to ions, $\mathcal{P}_p$, [11] does not significantly change T_e -behavior near the Earth; taking into account the spiral angle of the interplanetary magnetic field that decreases the radial heat flux in the solar wind, leads to even slower T_e decrease for r = 1 a.e. [12] as compared with [9, 11] . The similar conclusion on the 'spiral angle' effect on the radial temperature distribution in the solar wind was made based on one-fluid models [23, 24] .

With the coefficient of electron heat conduction in Cuperman and Hartle [16] and in Wolff, Brandt and Southwick [17] models that is lower than a classical coefficient, T_e decrease rate increases ($m \sim 0{,}6$ [16] and $m \sim 1$ [17]). That increase of $T_e(r)$ [16, 17] agrees with a faster T_e -decrease ($m \sim 0{,}5$) observed in the experiment on Mars-3 (chang-

ing the free parameter ρ [17] can obviously result in a quantitative agreement). In those models higher $T_e(r)$ is provided by introducing phenomenological coefficients (α , β , γ in [16] and (r/r_0) ρ in [17] , that do not describe physical processes leading to the decrease of electron heat conductivity.

Up to now some mechanisms have been proposed that do not exclude each other and explain the decrease in electron heat conductivity as compared with the conventional value. The asymmetry of the function of electron and ion distribution in the solar wind, caused by substantial heat flows in it and resulting in various kinds of plasma instabilities is discussed in [25] . Waves excited by these instabilities bring about stronger ion heating and lower electron heat-conductivity. The same effect is produced [26] by introducing of limited periodic motion of electrons that are reflected, along their path from the Sun, at the electrostatic barrier, the latter being the result of charge separation in the plasma, and along their pat. to the Sun at the 'magnetic mirror'. An additional mechanism that decreases electron heat conductivity and takes into account the intertangling of interplanetary magnetic field lines was proposed in [27] .

The development of the physical theory of transport processes that takes into consideration plasma instabilities due to substantial heat flows in the solar wind in the conditions of highly non-equilibrium functions of electron and ion distribution as well as the development of a solar wind model based on that theory will obviously result in an adequate understanding of processes in the interplanetary space.

FIGURE CAPTIONS

Fig. 1 Radial dependence of temperature of electrons (T_e) and protons (T_p) in the solar wind model of [9].

Fig. 2 The same as in Fig. 1 for the model of [11].

Fig. 3 The same as in Fig. 1 for the model of [12].

Fig. 4 The same as in Fig. 1 for the model of [16].

Fig. 5 The same as in Fig. 1 for the model of [17].

Fig. 6 Principal scheme of the "Mars-5" electron trap:
1 - body; 2 - gills; 3-4 - analyzing grids;
5 - electrostatical screen; 6 - collector.

Fig. 7 Electron temperature averaged over 3-hour intervals of time

Fig. 8 Histogram of the electron temperature values at the various distances from the Sun.

Fig. 9 Heliocentric distance to the "Mars-3" at the flight trajectory.

Fig. 10 The dependence of T_e on heliocentric distance:
——— according to the "Mars-3" data;
---- $T_e \sim r^{-2/7}$

REFERENCES

1. K.I. Gringauz, M.I. Verigin. Doklady AN SSSR 223, 77, 1975
2. M D. Montgomery, S.J. Bame, A.J. Hundhausen, J. Geophys. Res., 73, 4999, 1968
3. J.D. Scudder, D.L. Lind, K.W. Ogilvie, J. Geophys. Res., 78, 6535, 1973
4. W. Feldman, J.R. Asbrige et al., J. Geophys. Res., 78, 3697, 1973
5. E.N. Parker, in "Solar Wind", p. 161, NASA SP-308, Washington, 1972.
6. M.D. Montgomery, in "Cosmic plasma physics", p. 61, Plenum press, New York, 1972.
7. A.J. Hundhausen, "Coronal expansion and solar wind", Springer-Verlag, New York-Heidelberg-Berlin, 1972.
8. P.A. Sturrock, R.E. Hartle, Phys. Rev. Letters, 16, 628, 1966
9. R.E. Hartle, P.A. Sturrock, Astrophys. J., 151, 1155, 1968
10. S.I. Braginskii, Reviews of plasma physics, New York: Consultans bureau, 1, 205, 1965
11. R.E. Hartle, A. Barnes, J. Geophys. Res., 75, 6915, 1970
12. J.V. Hollweg, Astrophys. J., 181, 547, 1973
13. J.W. Belcher, L. Davis, Jr., J. Geophys.Res., 76, 3534, 1971
14. A.J. Hundhausen, J. Geophys. Res., 74, 5810, 1969.
15. S. Cuperman, A. Harten, Astrophys. J., 163, 383, 1971
16. S. Cuperman, A. Harten, in "Solar wind", p. 244, NASA SP-30 Washington, 1972.
17. C.L. Wolff, J.C. Brandt, R.G. Southwick, Astrophys. J., 165, 181, 1971.

18. K.I. Gringauz, V.V. Bezrukikh et al. Kosmicheskie Issledovanija, 12. 430, 1974

19. K.I. Gringauz, V.V. Bezrukikh et al. Kosm. Issledovanija, 12, 585, 1974

20. J.H. Wolfe, in "Solar Wind", p. 170, NASA SP-308, Washington, 1972.

21. P.J. Coleman, Jr., E.J. Smith et al., J. Geophys. Res., 74, 2826, 1969

22. M. Neugebauer, C.W. Snyder, J. Geophys. Res., 71, 4469, 1966

23. R.A. Gentry, A.J. Hundhausen, Trans. A.G.U., 50, 302, 1969

24. S. Cuperman, N. Metzler, Astrophys. J., 182, 961, 1973.

25. D.W. Forslund, J. Geophys. Res., 78, 17, 1970.

26. F. Perkins, Astrophys. J., 179, 637, 1973.

27. J.V. Hollweg, J.R. Jokipii, J. Geophys. Res., 77, 3311, 1972.

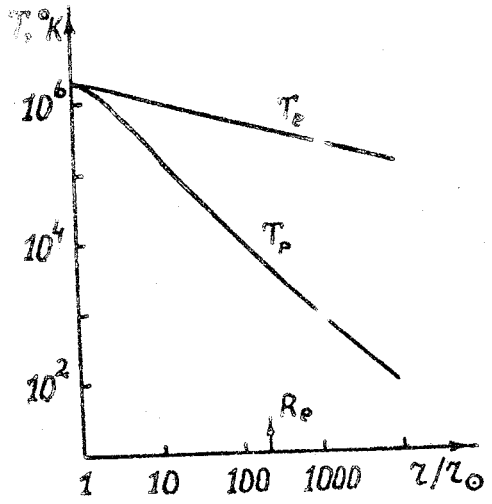
T, °K
10^6
10^4
10^2
T_e
T_p
R_e
1
10
100
1000
r/r_⊙

Fig. 1

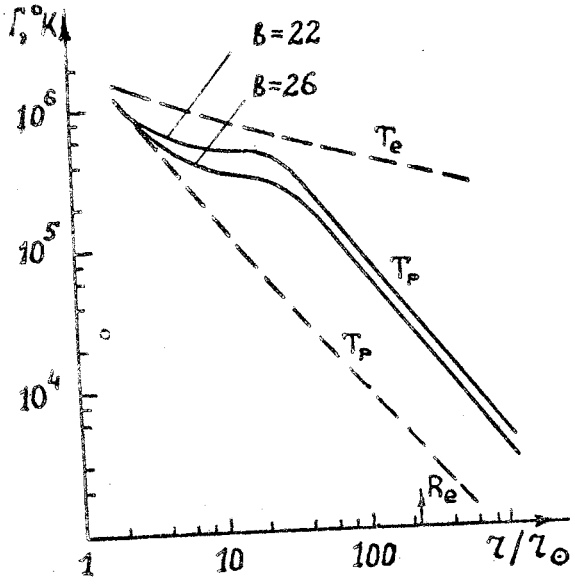
T, °K
10^6
10^5
10^4
B=22
B=26
T_e
T_p
T_p
R_e
1
10
100
r/r_⊙

Fig. 2

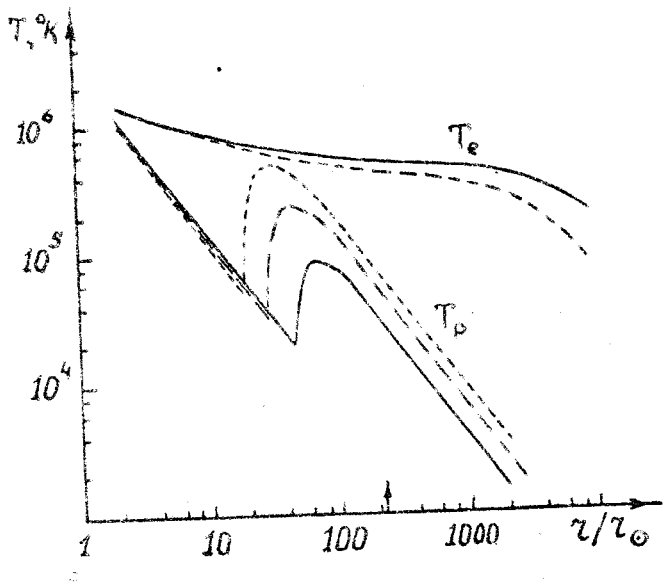
T, °K
10^6
10^5
10^4
T_e
T_p
1
10
100
1000
r/r_⊙

Fig. 3

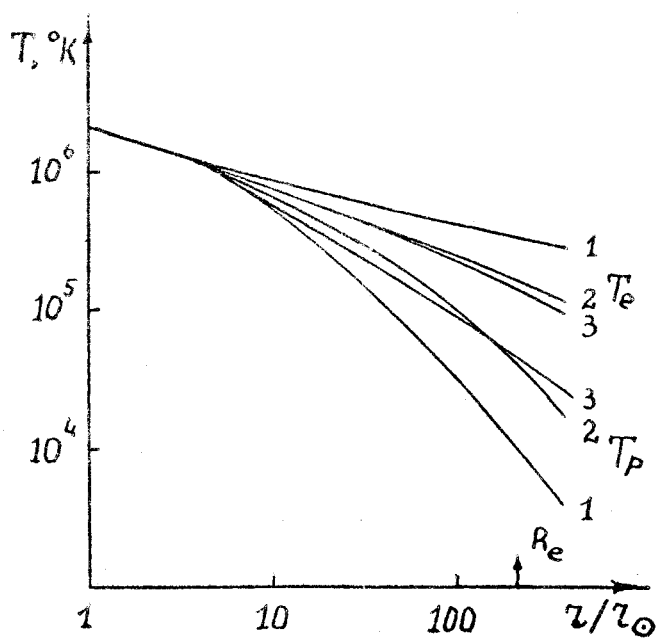
T, °K
10^6
10^5
10^4
1
2
3
T_e
3
2
T_p
1
R_e
1
10
100
r/r_⊙

Fig. 4

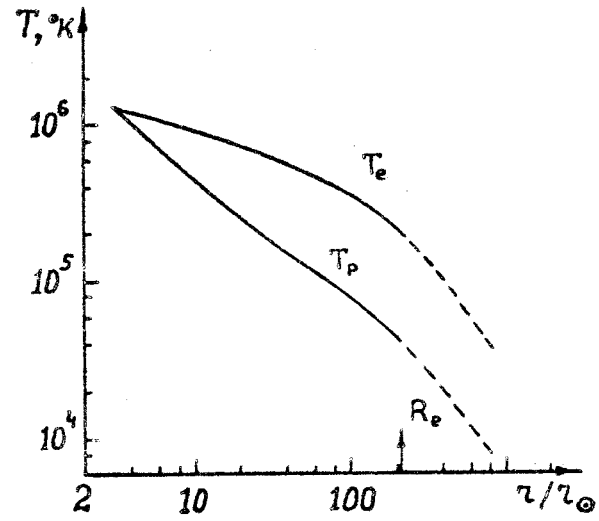

Fig. 5

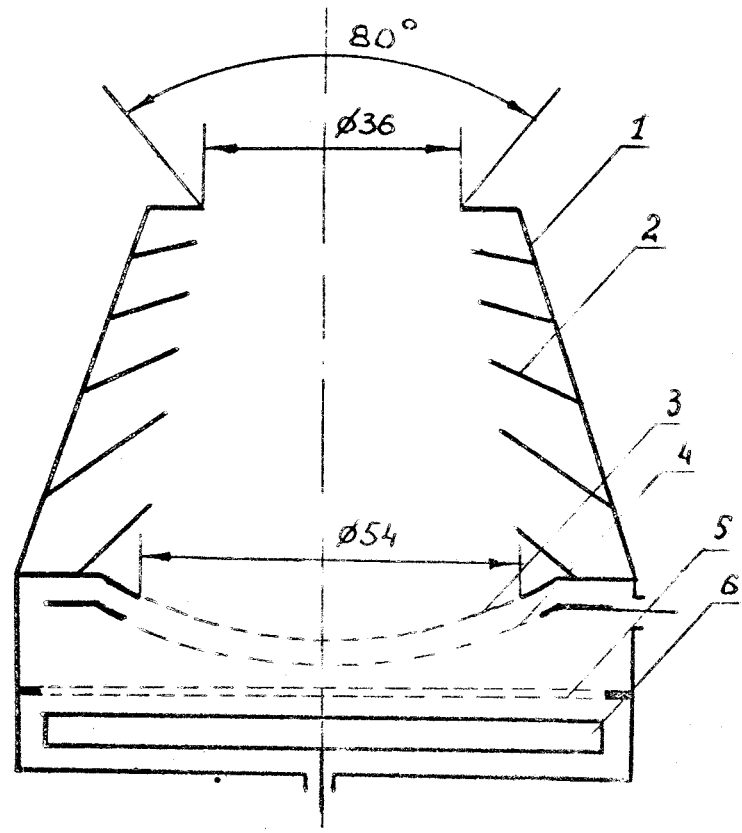

Fig. 6

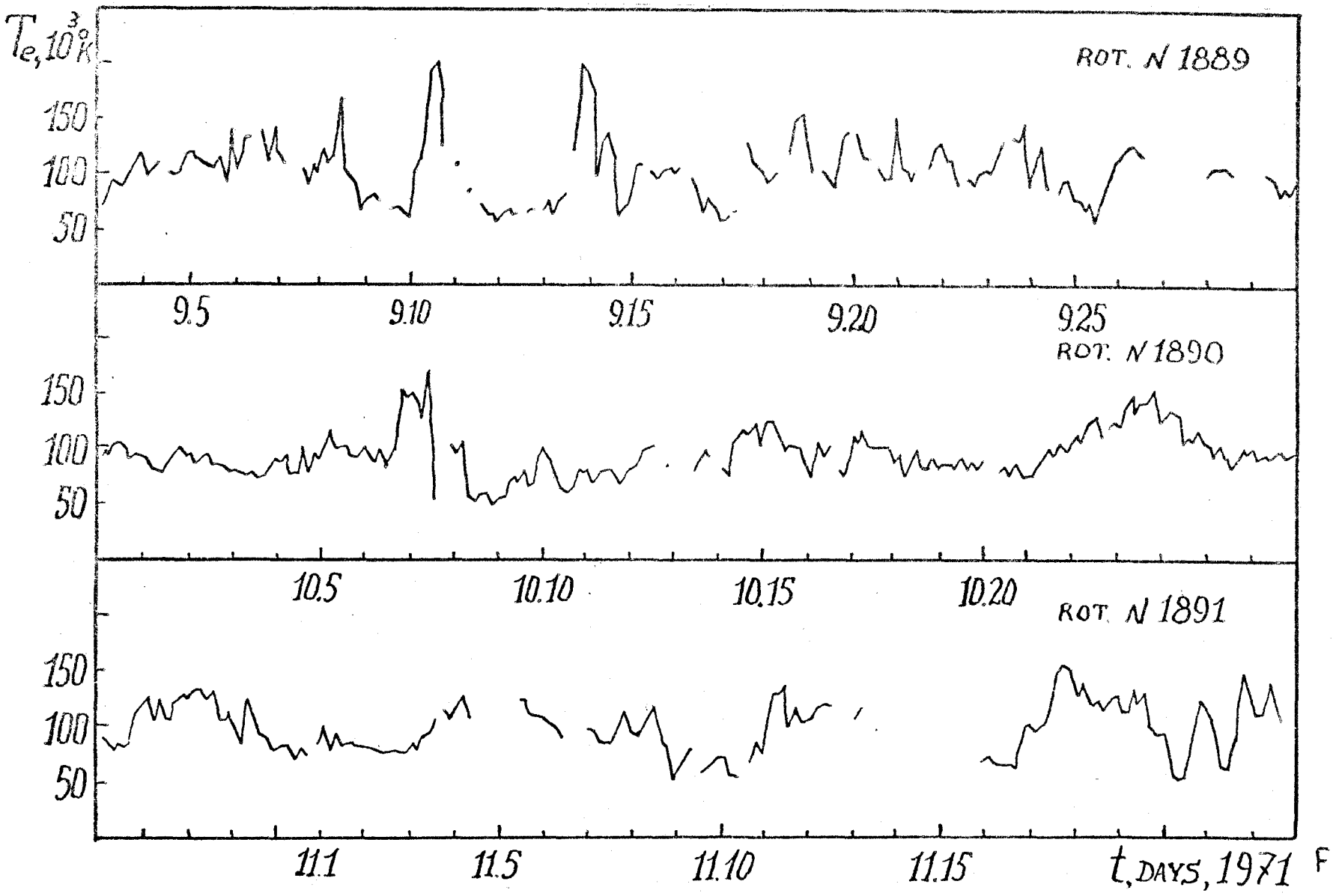
$T_e, 10^3$°K
ROT. N 1889
150
100
50
9.5
9.10
9.15
9.20
9.25
ROT. N 1890
150
100
50
10.5
10.10
10.15
10.20
ROT. N 1891
150
100
50
11.1
11.5
11.10
11.15
t, DAYS, 1971

Fig 7

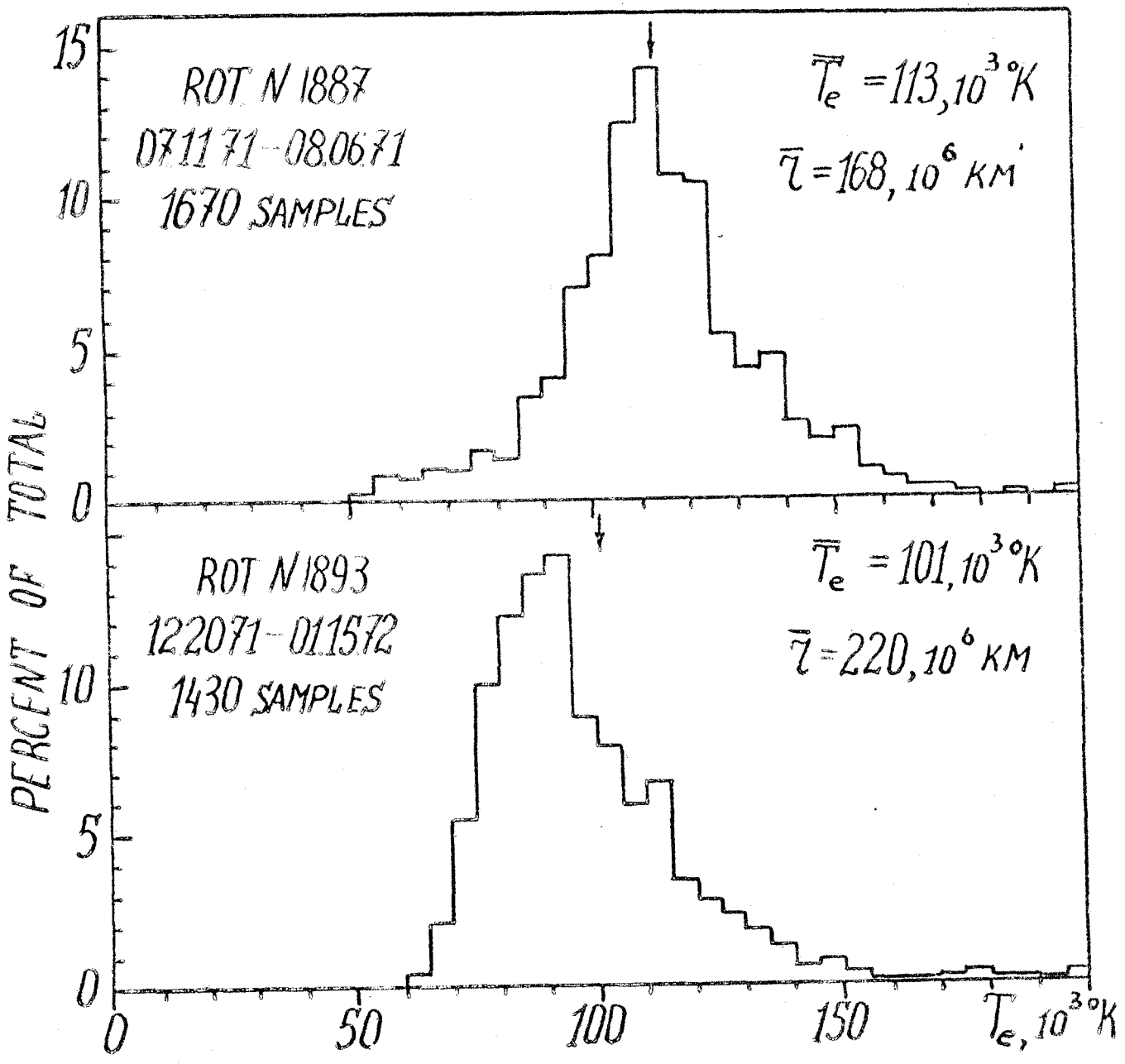
ROT N 1887
071171 - 080671
1670 SAMPLES
$\bar{T}_e = 113, 10^3 °K$
$\bar{\tau} = 168, 10^6$ KM
ROT N 1893
122071 - 011572
1430 SAMPLES
$\bar{T}_e = 101, 10^3 °K$
$\bar{\tau} = 220, 10^6$ KM
PERCENT OF TOTAL
15
10
5
0
10
5
0
0
50
100
150
$T_e, 10^3 °K$

Fig 8

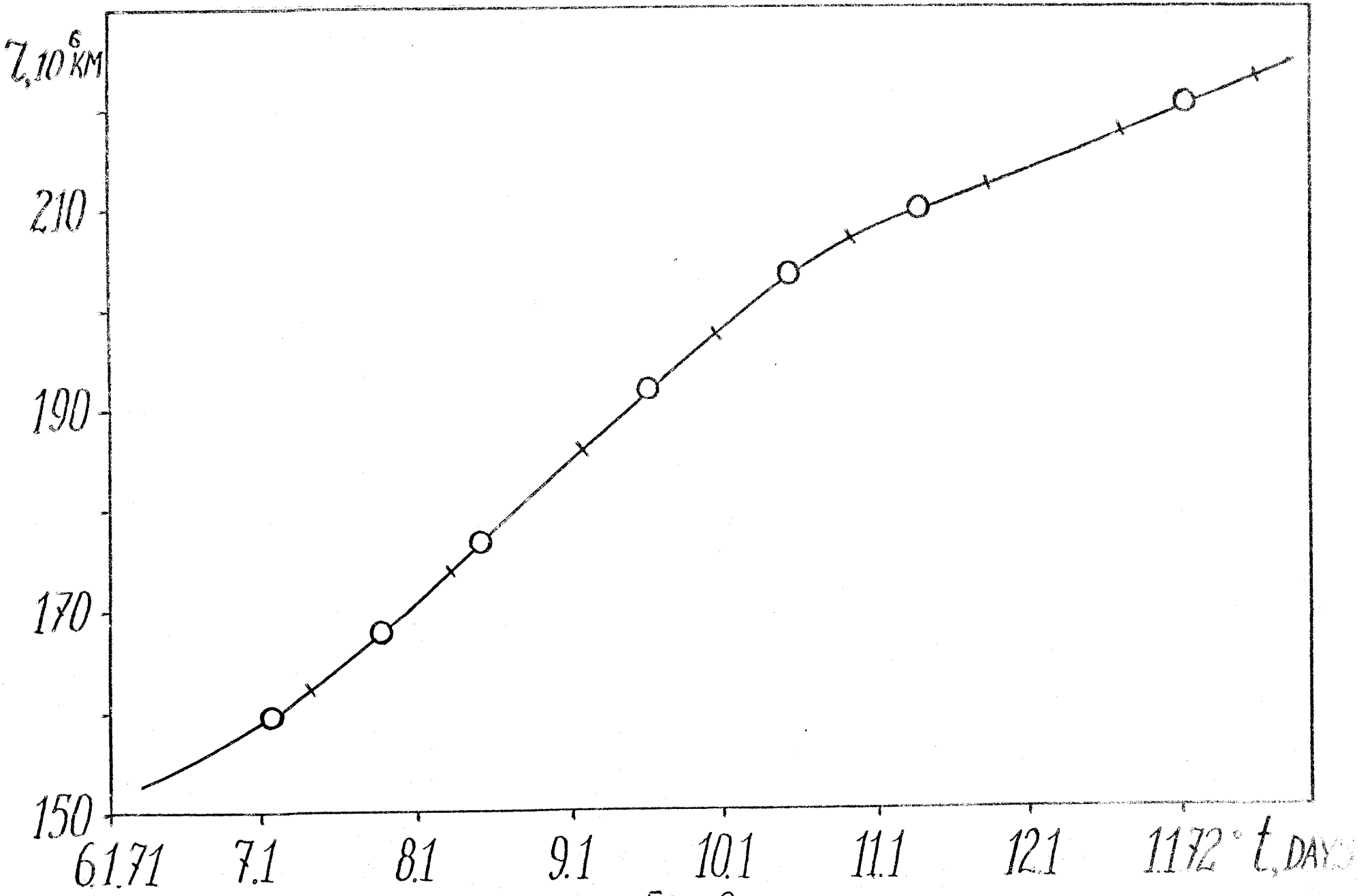

Fig 9

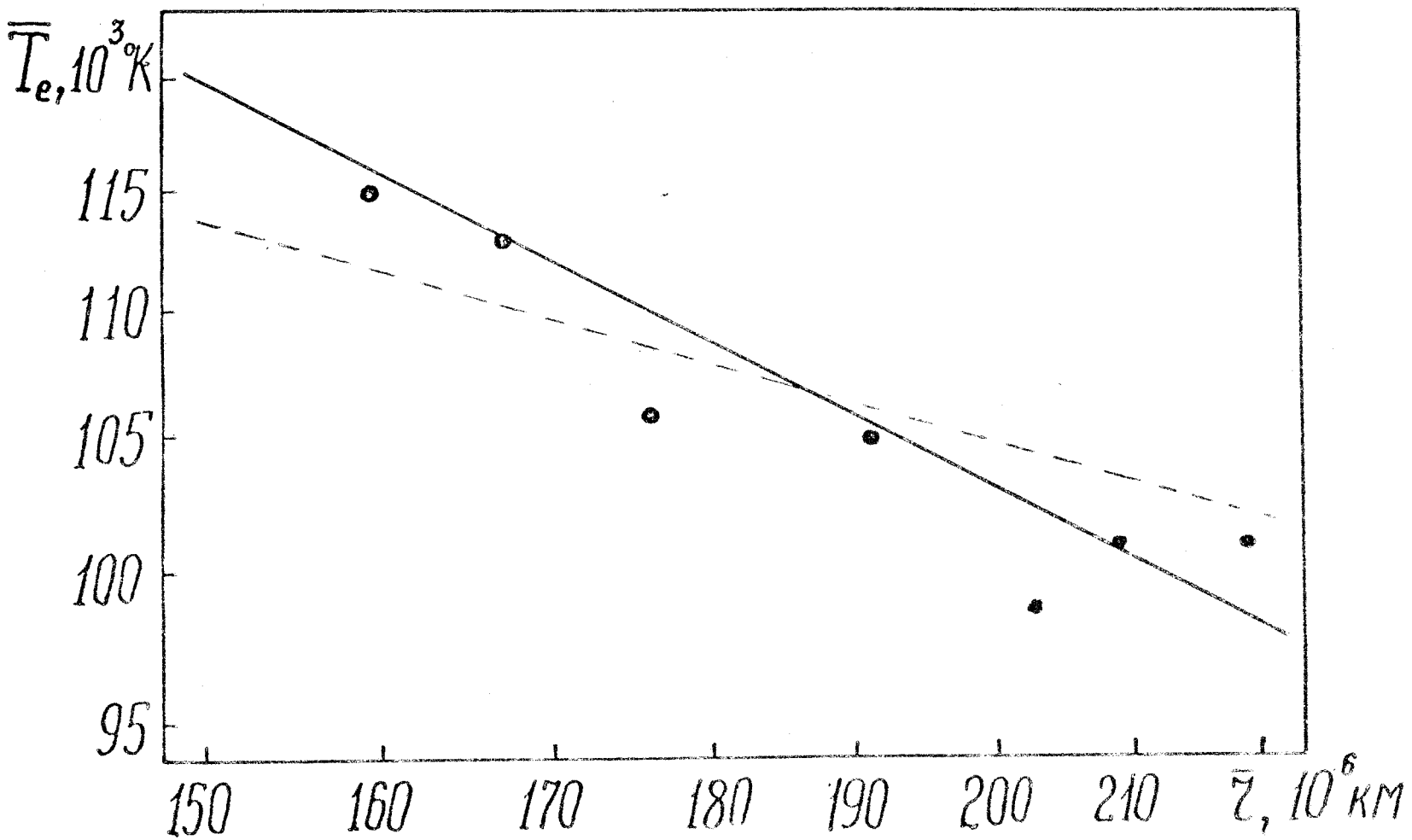
$\overline{T}_e, 10^3$°K
115
110
105
100
95
150
160
170
180
190
200
210
$\overline{z}, 10^6$ км

Fig. 10

055(02)2 Отпечатано в ИКИ АН СССР

Т-I3646 Подписано к печати I2.08.75

Заказ 3I3 Тираж I50 Объем I,I уч.-изд.л.